Microbial fuel cell as battery range extender for frugal IoT

Carlos Augusto Berlitz, Andrea Pietrelli, Fabien Mieyeville, Gaël Pillonnet, Bruno Allard

energies

MDPI

Article

Microbial Fuel Cell as Battery Range Extender for Frugal IoT

Carlos Augusto Berlitz [1,2,‡], Andrea Pietrelli [2,‡], Fabien Mieyeville [2,‡], Gaël Pillonnet [1,‡] and Bruno Allard [2,†,‡,*]

[1] CEA-Leti, Université Grenoble Alpes, F-38000 Grenoble, France; c.augustoberlitz@gmail.com (C.A.B.); gael.pillonnet@cea.fr (G.P.)
[2] Université de Lyon, INSA Lyon, Université Lyon 1, Ecole Centrale de Lyon, CNRS, Ampère, UMR5005, F-69621 Villeurbanne, France; andrea.pietrelli@univ-lyon1.fr (A.P.); fabien.mieyeville@univ-lyon1.fr (F.M.)
* Correspondence: bruno.allard@insa-lyon.fr; Tel.: +33472438238
† Current Address: INSA Lyon, 21 avenue Jean Capelle Ouest, F-69621 Villeurbanne, France.
‡ These authors contributed equally to this work.

Abstract: The simplest DC/DC converter for supplying an Internet-of-Things device is definitely a switched-capacitor converter. The voltage from a mere 1.2 V battery may be stepped up to 2 V. A quite large operating frequency is required in order to reach the smallest possible output impedance value of the DC/DC converter. The overall efficiency is then limited even more so if the power area density of the system should be large. The article details how a microbial fuel cell may substitute one capacitor in the switched-capacitor converter, achieving a better efficiency at a much lower operating frequency. In that perspective, the microbial fuel cell acts as a kind of battery range extender. Some limitations exist that are discussed. A simple converter is experimentally evaluated to support the discussion. Substituting a microbial fuel cell inside a 100 µW switched-capacitor converter compensates for losses in the order of 5% of efficiency. Moreover, the microbial fuel cell extends the lifespan of the battery, as 1.6 V output voltage is still possible when the battery voltage drops to 0.8 V. More than 94% efficiency is measured for a range of output power between 100 µW and 1 mW, which is sufficient to address a lot of frugal IoT applications.

Keywords: DC/DC boost converter; switched-capacitor converter; microbial fuel cell; range extender

Citation: Berltz, C.A.; Pietrelli, A.; Mieyeville, F.; Pillonnet, G.; Allard, B. Microbial Fuel Cell as Battery Range Extender for Frugal IoT. *Energies* **2023**, *16*, 6501. https://doi.org/10.3390/en16186501

Academic Editor: Vedran Mrzljak

Received: 31 July 2023
Revised: 4 September 2023
Accepted: 7 September 2023
Published: 9 September 2023

1. Introduction

Supplying an Internet-of-Things (IoT) device has become an important issue for the sake of eliminating batteries. In extension, a dichotomy has appeared in the community between battery-powered and battery-less IoT.

The power supply of an IoT device is challenging for many reasons related to technology, physical deployment, constraints of environment, constraints of operation, etc. A strong research field is related to the challenge of autonomous IoT systems. In that perspective, energy harvesting is the primary solution, exploiting light, wind, vibration or temperature [1]. Looking closely at the IoT system, it is possible to select the electronic architecture and the operation mode so as to align the power consumption with the power and energy delivered by the energy-harvesting system [2]. The electronic part of the IoT system benefits from low-power integrated circuits whose consumption is ever reduced but at some point requires a certain energy and power budget [3]. The reliability of the system operation is at stake as well as the volume and weight of the solution. The literature lists numerous examples where the capabilities of the energy-harvesting approach and conversion schemes are analyzed and compared [4].

In a more radical approach of autonomy, battery-less IoT systems can be considered. In such configurations, operation is possibly intermittent, and the operation duty cycle is the factor that characterizes how unbalanced the load power consumption from the available power and energy delivered by the harvesting function may be. Intermittency is taken into account for optimizing electronic circuits or communication strategies [5] and benefits

to the rate of operation. Namely, the energy-harvesting function has to pump electrical energy into a capacitor until a sufficient level is reached that enables the operation of the IoT system for a certain amount of time. This depends on the context and the nature of ambient energy that is selected to supply the IoT device. Energy-harvesting systems based on solar light [6,7] and mechanical vibrations [4] deliver more power than ambient radiofrequency energy-harvesting solutions [8] or microbial fuel cells [9]. The thermoelectric approach [10] offers an intermediate level.

Delivering energy to a capacitive buffer prior to supplying the IoT device is the simplest way to disconnect the peak power need from the average energy budget required by a typical operation cycle of the device. The voltage across the capacitive buffer decreases during the IoT device operation until a low threshold limit is reached that stops the IoT device operation. It is difficult in that context to ensure the IoT device may operate at a specific time or during a specific amount of time unless increasing the complexity, size and weight of the harvesting function [2]. The capacitor value can be increased to alleviate such bottlenecks, but this impacts the volume and weight of the device. When the IoT device operation is mandatory at a specific time, the reliability dictates to adopt a more powerful source of income energy or to rely on a battery, rechargeable or not.

The specific power and energy densities of a battery are different if it is a rechargeable device. This is a reason why the so-called non-rechargeable coin battery is still popular in low-power IoT devices, although rechargeable coin battery is expending its usage [11]. As an example, the battery VARTA 344-SR42SW features 1.55 V open-circuit voltage. The internal impedance varies between 5 Ω and 100 Ω depending on the output peak current. The initial capacity is 100 mAh, and a zero state-of-charge corresponds to a residual open-circuit voltage of 0.8 V. The initial capacity is unfortunately not entirely consumed by the IoT device to supply. A DC/DC converter is necessary in between, and the converter efficiency is impacting at the first order. The battery itself is affected by internal Joule losses and by a small but measurable leakage current. In the example case (SR42SW), this is characterized by a nearly 200 nA leakage current. There is interest in introducing a secondary source of energy as a companion to the primary battery. To the best of the authors' knowledge, the combination of a primary (coin) battery and an energy-harvesting function has not been extensively reported. The intricate combination of an ambient energy-harvesting system with a storage element is seldom discussed as well [12], not like the association or addition of functions [13,14].

The integrated companion energy-harvesting function should act as a kind of range extender if the battery is not rechargeable. The term range extender exists for electrical vehicles [15] in which it refers to the increase of range (and then autonomy) of the vehicle (in terms of battery capacity) from an electrical point of view [16]. In an electric vehicle, the photovoltaic assistance is studied [17] as well as the hydrogen fuel cell [18]. The hydrogen fuel cell offers the advantage of smooth operation until the hydrogen tank is empty and a refill is necessary. There is no intermittency of the energy source. In the domain of wireless systems and a Wireless System Network (WSN), the term range extender is used to define the increase in the distance range of the communication, such as the LoRa solutions for example [1,19] or RFID-based solutions [16].

The paper discusses the transfer of the notion of a range extender, the prolongation of energy supply as evaluated in the electrical vehicles domain, to the domain of smart communicating systems such as IoT nodes, through the usage of microbial fuel cells (MFCs). The paper's objective is to present experimental observations of two kinds. The experiment is not about an electrical interface for scavenging energy directly from an MFC. It is not about a particular MCF technology, either. One aspect is that it is possible to substitute a capacitor in a switched-capacitor converter with an MFC. A second aspect is that the MFC delivers energy to the system, although the device operates in a non-standard condition from an electrical point of view.

As the MFC considered here acts as a reservoir of energy, Section 2 discusses the challenges of using the MFC as a primary source of electricity. Section 3 introduces a

specific DC/DC converter derived from the switched-capacitor DC/DC converter to use the MFC as a range extender. Section 4 details experimental measurements and discusses the limitations of the converter scheme.

2. MFC as Autonomous Solution to Supply IoT

The microbial fuel cell is a bio-electro-chemical system that hides a large variety of types [20] depending on the technology and the main substrate in which microorganisms (living species) take their nutrition, i.e., catalyze oxidation/reduction reactions through donor/accept electrons from an electrode. Namely, bacteria are used in many types of MFC technologies with liquid or solid (earth) substrate, or whatever material is suitable for bacteria development [21]. The paper considers here the case of batch-mode MFC as opposed to in-flow MFC. The MFC is then a sealed reactor where nutrients have been incorporated along with waste material or purposely with ad hoc chemical compounds.

Regarding the power supply of sensors, numerous contexts are considered with dedicated MFCs [22]. Benthic or sediment MFCs [9,23], plant MFCs [24] or waste-water-based MFCs [25] lead to different designs and consequently to specific electrical performances. In [26], the authors demonstrate a fully integrated solution based on a body-wearable bio-galvanic fuel cell. In each context, many studies report improvement of the power density of MFC reactors [27]. Using the cathode effective area as a reference metric, the power density varies roughly between 50 and 2000 mW/m^2. The open-circuit voltage ranges is well under the Volta potential (∼1.2 V), and it is typically between 0.4 and 0.8 V. When delivering an output current, the output voltage drops due to internal mechanisms. The reactor may be qualified by an effective internal impedance from several 10 s of Ohm to several 100 s of Ohm. It is possible to assemble MFCs to build a more complex power system: hence, association in parallel or a series of elementary MFC reactors permits achieving better peak voltage or power levels [28].

2.1. I-V Curve and Electrical Performances

Measuring the I-V curve of an MCF is quite a challenge. The potentiostat method [29] applies a defined resistive load at the MFC output and considers the variation of output voltage. Automated equipment is used to perform the measurements as detailed in [30]. The MFC used in the experiment is characterized in Section 3. Figure 1 shows that microorganisms inside the MFC reactor introduce particular time constants: MFCs generally do not react quickly enough to a sudden change in electrical conditions. It is possible to some extent to identify the main time constants using impedance spectroscopy [31].

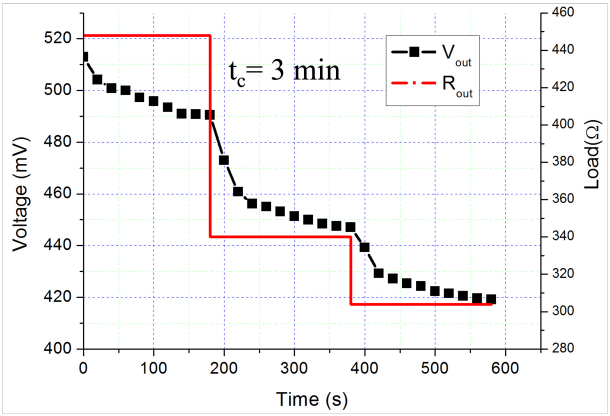

Figure 1. Electrical behavior of an MFC under sudden changes of the output resistive load. A 3 min delay is introduced between successive changes (single-chamber, batch-mode MFC of 0.7 dm^3 with wasterwater liquid substrate and nourished with 1 g/L of acetate).

Independently of the MFC technology, the I-V curve evaluation and the electrical behavior is similar to the one in Figure 2 where an output resistive load is swept and the

effective MFC output power is evaluated. The output voltage in open circuit conditions is typically in the range 0.2 to 0.8 V in nominal conditions, and a simple MCF reactor will exhibit 0.8 V (wastewater, 1 g/dm^3 acetate). The internal impedance is in the range 100 Ω to 1000 Ω (for a classical wastewater, single-chamber batch-mode reactor MFC).

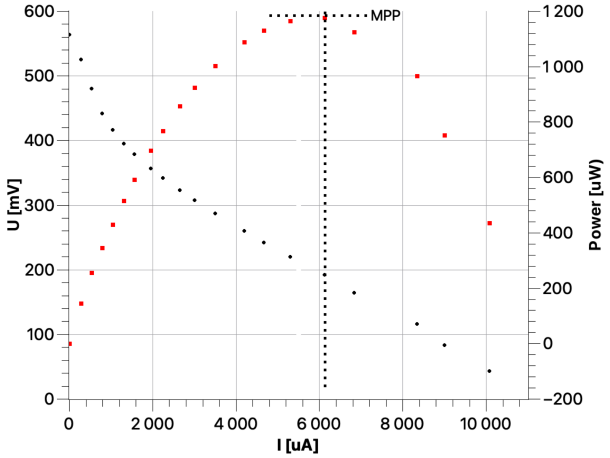

Figure 2. I-V characteristic of a single-chamber, batch-mode MFC of 0.7 dm^3 with wasterwater liquid substrate and nourished with 1.5 g/L of acetate.

The internal impedance seen from the electrical output is a major constraint on the electrical interface for energy scavenging because of the necessity for an adaptation of impedance to optimize power transfer from source to load. An MFC presents a low open-circuit voltage worsened by the fact that the electrical performances are degraded when the batch-mode MFC weakens.

Over time, microorganisms consume the available nutrients, and the oxidation/reduction reactions slow down. The consequence is a slower transit flow of ions inside the substrate and a lower number of donor/accept electrons. This is visible in Figure 3 where nutrients come from acetate with different density. It is particularly the case for batch-mode reactors, but the situation may appear in many other types of MFC. Figure 3 shows how the weakness of a typical MFC affects the electrical performances. Temperature may also affect in a similar manner the electrical performances. At some point, the open-circuit voltage and/or the Maximum Power Point (MPP) value are not sufficient to permit a standard electrical interface to operate. This case of weak MFC is one focus of this paper.

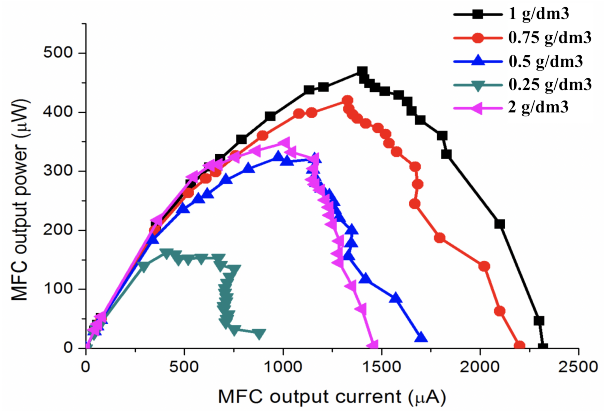

Figure 3. Electrical performances of a batch-mode MCF with various level of acetate density.

2.2. Electrical Interface

As introduced in Section 1, scavenging energy requires installing Maximum Power Point conditions: the electrical interface connected to the MFC should present an input impedance of the same value as the MFC effective internal impedance. The literature

details several topologies of the DC/DC converter dedicated to energy harvesting [32–35]. In [35], the authors demonstrated that a BQ25505 IC associated with the TPS61200 IC produces an electrical interface with an efficiency of 59.6% but requires an input voltage larger than 236 mV. The BQ25505 IC from Texas Instruments is an ultra-low-power battery lifter and charger specialized in medium-impedance low-power sources (maximum 100 Ω). The TPS61200 IC from Texas Instruments is a high-efficiency synchronous DC–DC boost converter with a configurable output voltage from 1.8 to 5.5 V. Ref. [9] considers a supercapacitor system to accumulate the energy from a single-chamber MFC in batch mode. Multiple configurations (single, parallel or series) are evaluated using two classical power-management solutions (LTC3108 IC and BQ25504 IC). The efficiency spans from 4.56 to 85.45%. The intermittency of the sensor operation in [35] is not discussed as in [9], but the balance of energy shows that a continuous operation is not possible with the proposed energy-scavenging scheme.

Other commercially available integrated circuits exist (AEM10941 E-PEAS, NH2D0245 NOWI, CITIUS CHIP) with more or less similar limitations: a significant open-circuit voltage for start-up and an MPP scheme that is not particularly adapted to the MFC dynamic behavior. The MPP scheme is periodically activated but with a delay, which is way too short compared to the MFC time constant (Figure 1).

The serial association of MFCs is meant to increase open-circuit voltage. It has been covered in the literature, and an active balance scheme is mandatory to tackle the variability between individual MFCs. These approaches result in establishing a voltage source with a larger open-circuit voltage but at the penalty of a significant internal impedance.

Furthermore, a lot of effort addresses the miniaturization of the DC/DC converter either using 3D silicon capacitors in the case of a switched-capacitor voltage converter or 3D inductance in the case of a magnetic voltage converter. Mimicking a specific input inductance is the main feature of a Flyback DC/DC converter as shown in Figure 4, preferably operating in discontinuous conduction mode [26,36]. The Flyback main transistor, M in Figure 4, requires a nominal gate voltage that one MCF is not able to deliver alone. The system may not start by itself unless a so-called cold-start function is implemented. The cold start-up issue of the experimented circuit in Section 3 is out of the scope of this paper. An oscillator is generally used for that purpose, and a so-called Amstrong configuration is traditionally used (as shown in Figure 4). Using a bulky coupled-inductor, the magnetic device (L_{Rp}-L_{Rs}) enables charging the capacitor C_{out} to a near sufficient voltage to operate the transistor M gate in the Flyback. The bias consumption of the transistor M gate controller adds steady-state losses and the minimum cold start-up voltage is reported to be in the range of 120 to 180 mV in the literature.

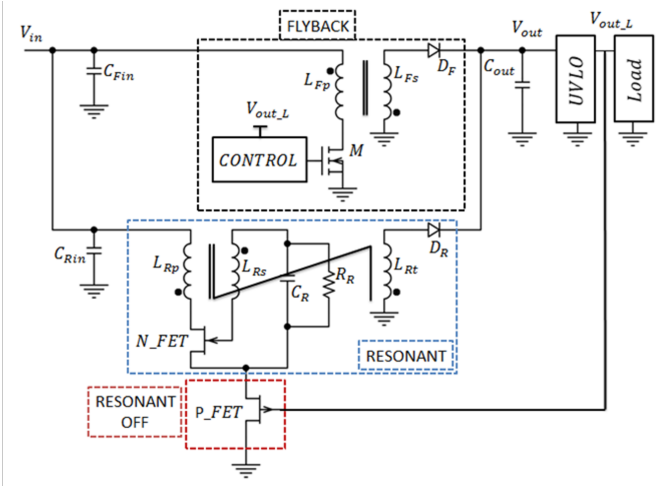

Figure 4. Flyback converter in discontinuous-conduction mode assisted by an Amstrong oscillator as a cold starter.

The circuit in Figure 4 operates the MPP conditions for optimal energy harvesting using the fractional open-voltage circuit scheme. It is an open-loop approach that becomes unsatisfying if the MFC weakens: the MFC open voltage may drop below the minimum sustaining value to keep the Flyback in operation (90 mV reported in the literature).

As a conclusion, an MFC is able to supply an ultra-low-power IoT system, but continuous operation may be difficult to secure. A group or plant of MFCs may be sufficient, but the system becomes bulky. Section 3 introduces a simple DC/DC converter where one MFC is introduced to compensate for part of the losses of a converter supplied by a non-rechargeable battery. This is particularly interesting when the primary source is a tiny battery to extend its lifespan.

3. Switched-Fuel-Cell Converter

The concept of a switched-capacitor converter (SCC) has been extended to batteries [37]. The main interest is that the effective efficiency is enhanced at very low switching frequency. A tiny charge exchange is operated within the battery. The present study explores the possibility of substituting the battery by one MFC in the topology in [37].

3.1. Switched-Battery Converter

Supplying an IoT device from a low-voltage input source requires a boost DC/DC converter. The simple voltage-doubler converter is considered. A supply voltage of 2 V at least comes in a straightforward manner from a 1.2 V input battery.

The voltage doubler is the standard topology of a switched-capacitor converter [38,39]. The circuit in Figure 5 consists of two capacitors and four switches. The converter operation is composed of two phases of similar duration and repeated at an operating frequency, f_{sw}. In a first step, the so-called flying capacitor, C_{FLYING} is connected to the input voltage, V_{IN}, with switches S_1 and S_4 (switches S_3 and S_2) opened. The flying capacitor charges to V_{IN}. In a second step, the flying capacitor is then connected in series with V_{IN} to boost the voltage across the capacitor C_{OUT}. The output voltage V_{OUT} ideally reaches twice the input voltage amplitude.

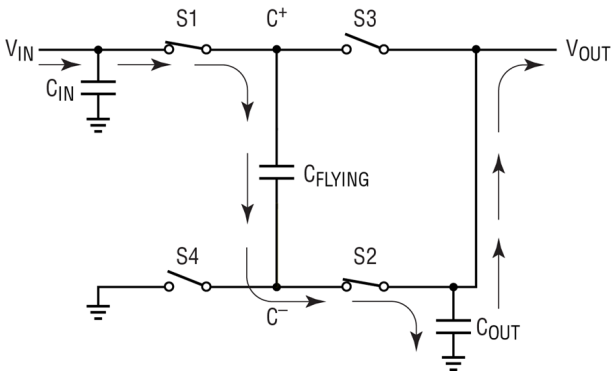

Figure 5. Typical voltage-doubler SC converter.

The flying capacitor may be replaced by a rechargeable battery in a classical 2:1 configuration (Figure 5). The operation is similar to that of the original voltage doubler. The lab-scale implementation in [38] uses a commercial LM2663 circuit from Texas Instruments. The results show a superior efficiency of the switched-battery converter (SBC) over the switched-capacitor converter.

The most interesting results in the switched-battery voltage doubler are the following ones:

- Cycling a rechargeable battery at 100 Hz does not impact the battery lifespan.
- In steady state, the battery voltage copies the input voltage amplitude, although it is different from the nominal value.

- The output voltage ripple remains acceptable even at very low operating frequency (1 Hz).

One motivation behind the work was to observe if an MFC could also operate in substitution of the flying capacitor.

3.2. Novel Proposed Voltage-Doubler Topology

The study considers a scenario where one MFC supports a principal source of voltage (non-rechargeable battery coin). The latter source could be also an MFC, but it is not evaluated here. The study focuses on the system operation when the flying MFC may become weak for evaluating if further energy is scavenged from this MFC and up to what level. The converter schematic is pictured in Figure 6. The topology is called a switched-fuel cell (SFC).

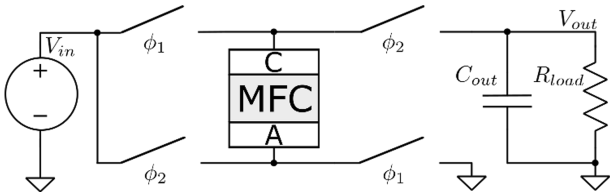

Figure 6. Switched DC/DC voltage doubler using a flying MFC.

The operation of the proposed SFC is inherited from the previous one (SBC), pictured in Figure 7, which is detailed here-before:

- During phase φ_1, the MFC receives a tiny amount of charge, +Qe. Despite the MFC's initial open circuit voltage (V_{OC} < 600 mV) being significantly low, the MFC reaches an operating point where its effective voltage is close to the voltage imposed by the principal voltage source. An MFC features a capacitive behavior related to its electrical electrodes.
- During phase φ_2, the principal voltage source and the MFC deliver in series an amount of charge to the output capacitor and load. As a steady state is reached, the latter amount of charge is equal to +Qe. Hence the MFC delivers an amount of charge −Qe to the circuit. The implemented SFC converts a principal input voltage (V_{in}) into an output voltage of nearly twice the amplitude when operating at a switching frequency of 10 Hz, 100 Hz or 1 kHz.

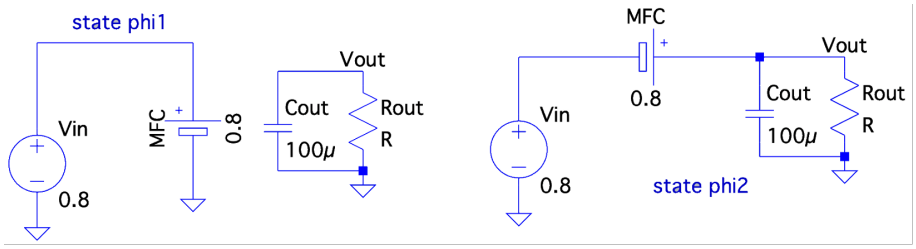

Figure 7. Operation of the circuit.

4. Experimental Results

With an input voltage, V_{in} of 1.2 V, the switched-fuel cell voltage doubler produces an output voltage of 2.4 V. This is not an unexpected result, as there are similarities between the SFC and the SBC. More interestingly, it is important to verify if the SFC operation is altered when the input battery coin voltage decreases and in the presence of a weak MFC. The scenario corresponds to the end of the energy autonomy: the battery state-of-charge is low and the MFC is becoming weak.

A weak MFC is unsuited for the use as an energy source by itself. Considering the weak MFC as the unique source to keep supplying a payload does not make sense. However, the SFC concept enables scavenging more energy from the MCF than any other

electrical interface mentioned earlier. The reason is the MFC output voltage decreasing below a threshold value. This limitation is not applicable in the SFC.

Experimentally, the circuit is implemented using the popular circuit driver LM2663 from Texas Instruments as indicated in Figure 8.

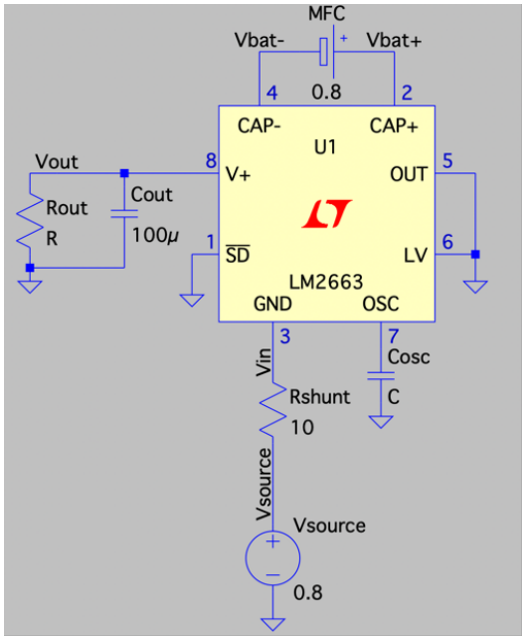

Figure 8. LM 2663 circuit system configuration.

The testbench is pictured in Figure 9 where a depleted MFC is implemented (open voltage below 300 mV). The principal voltage source is a low-impedance power supply (800 mV, 50 Ω) mimicking a depleted battery coin. The LM2663 driver necessitates a small capacitor C_{osc} in Figure 8 to tune the switching frequency between 1 and 10 kHz according to Table 1.

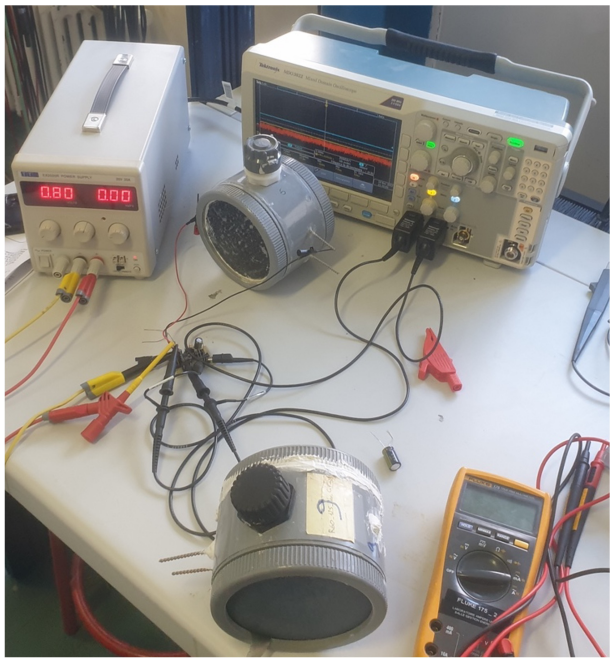

Figure 9. Testbench with the circuit: a lab-scale, batch mode, one-chamber depleted MFC is implemented.

Table 1. C_{osc} capacitor value for operation of LM 2663.

Frequency (Hz)	4.2	10	100	1 k	10 k
Capacitor (nF)	800	405	25.5	3.5	0.4

The LM2663 driver absorbs a bias current depending on the effective output voltage. The datasheet gives nearly 25 µA at 1.5 V output voltage. If the battery coin would be implemented inside an SCC voltage doubler, the bias current would have a severe impact on the efficiency in normal operating conditions (small steady-state output current absorbed by the IoT device and nearly 100 µA bias current at 2.4 V output voltage).

4.1. Cold Start

The cold-start conditions of the system in Figure 8 are not evaluated. The output capacitor, C_{out}, is precharged to 1.6 V prior to any evaluation. The input voltage is fixed to 800 mV to figure out a scenario where the primary battery (coin) becomes depleted. It is a long-term condition and it is considered that the system remains in operation while the input voltage decreases.

The IC LM2663 requires a minimum voltage of 1.2 V for a correct start-up. These conditions are not met here from a strict point of view, and precharging the output capacitor is a quick manner to overpass the startup issue.

4.2. Operation

For any selected operating frequency, a sufficient time is allowed for the output voltage to reach a steady-state value. Said otherwise, the depleted MFC enters a transient behavior until its output voltage settles to 800 mV, which is the voltage imposed by the principal source. The current I_{out} in the $load_{out}$ varies between 30 µA and 1 mA depending on the experimental conditions. The efficiency is evaluated based on the current delivered by the principal source thanks to a shunt resistor of 10 Ω (Figure 8).

The MFC absorbs an amount of energy during phase φ_1 of operation and desorbs another amount of energy during phase φ_2. The central question is to evaluate if the effective action of the MFC is equivalent to that of a passive capacitor or if energy is scavenged from the MFC during the operation. The answer to the question resumes in comparing the SFC operation to that of an equivalent SSC. The equivalent capacitance of the MFC is not easy to determine, as the equivalent SCC should be designed with such a capacitor value. Successive design iterations are necessary to decide on a suitable capacitor value.

Figure 10 shows a primary comparison between the SFC with a weak MCF and an SCC with a capacitor of 110 µF at 4.2 Hz operating frequency. The ratio $\eta = \frac{V_{out}}{V_{in}}$ gives the energy efficiency of the SCC but not for the SFC, as the MFC should be accounted for. For comparison purposes, the metric is used from the point of view of the main coin battery. The metric reflects the level of losses dissipated in the converter. The metric is called partial efficiency for the SFC. The large capacitor value seems to corroborate the capacitive behavior of the MFC from an impedancemetry point of view.

At low frequency, the internal impedance of an SCC is quite high; thus, the efficiency is expected to decrease with a larger output current amplitude. The SFC does not present a similar behavior, which proves two issues:

- The MFC does not operate in the circuit as a mere capacitor, similarly to the battery in the SBC topology.
- The MFC, although weak, is able to provide a certain amount of energy to the converter as the coin battery has less energy to deliver to the system.

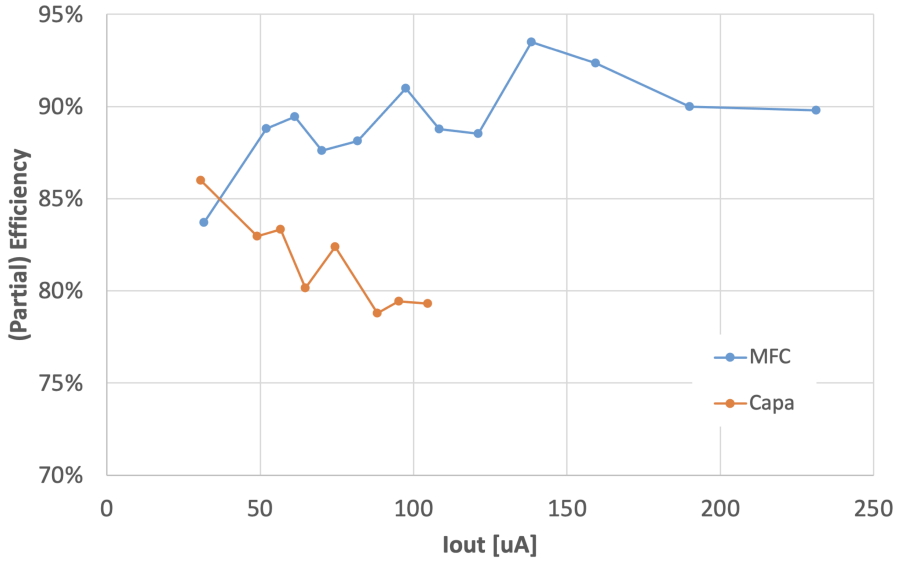

Figure 10. Comparison between an SFC and an SCC with corresponding conditions and at 4.2 Hz.

4.3. Impact of the Operating Frequency

The SFC with the depleted MFC reaches a maximum output power of 1.4 mW maintaining a high efficiency (>90%). It also manages to hold a high partial efficiency (>95%) for an output power range greater than 1.2 mW and reaches a peak partial efficiency of 97.25% at 100 Hz (Figure 11). The output power range with an effective partial efficiency >94% goes from 0.2 to 1.2 mW. When compared to an SCC under equivalent conditions, the SFC presents a better operation than the SCC counterpart from the coin battery lifespan perspective. Whatever the flying capacitor, the obtained SCC efficiency is always lower. Moreover, a reduced output voltage ripple is observed in the SFC if the operating frequency is higher than 10 Hz. From these observations, it appears that the MFC does not behave strictly like a passive capacitor, and some amount of energy is scavenged in the operation as the partial efficiency is somewhat higher than in an SSC. From that perspective, the MFC acts more as a range extender of the primary battery than an auxiliary energy source.

The results show that a weak MFC can successfully be used in the SFC, as some amount of energy is scavenged. The electrical performances of the depleted MFC create a difficult situation with regard to standard interface circuits devoted to energy harvesting as mentioned in the introduction, should the MFC be used in a straightforward manner. The SFC topology helps overcome this limitation.

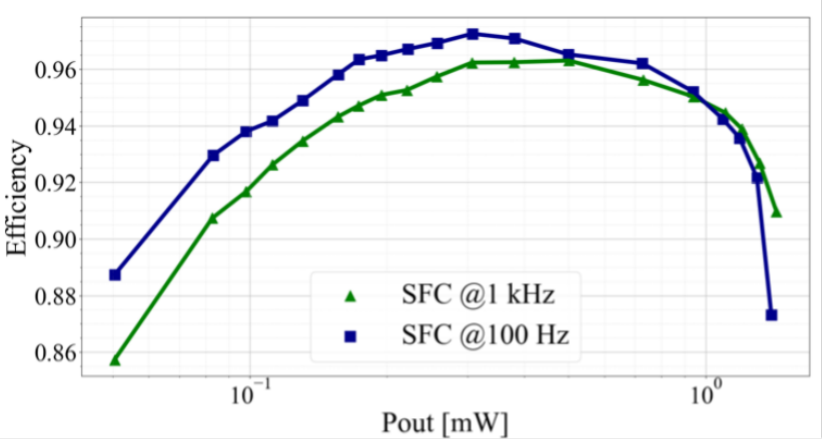

Figure 11. Partial efficiency of the voltage-doubler SFC against output power at 100 z and 1 kHz.

There is an impact of the operating frequency on efficiency (Figure 12). Unexpectedly, a lower frequency has an impact on the LM2663 driver as the static consumption should be lower. However, the circuit managed higher than 90% partial efficiency at 10 Hz for P_{out} from 155 µW up to 814 µW. And for Pout of only 50 µW, there is still a partial efficiency of over 75% at 10 Hz .

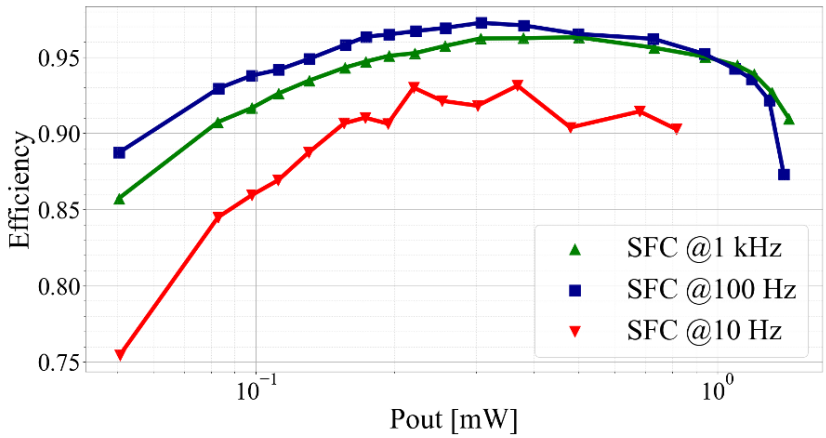

Figure 12. Impact of the operating frequency on partial efficiency.

4.4. Ripple

As expected, the ripple value increases with low frequencies (Figure 13). Larger ripple values also impact the higher output power for each frequency. At 4.2 Hz, P_{out} reaches 342 µW, and the ripple represents 7.8% of the output voltage. At 10 Hz, P_{out} reaches 841 µW, and the ripple represents nearly 10% of the output voltage. At higher operating frequency, the ripple drops below 0.6%, which is a satisfying value. Unfortunately, the output power culminates at 1.4 mW at 100 Hz and 1 kHz, respectively. So, there is a "kind of" optimal operating frequency with respect to the maximal output power (for which unfortunately the ripple is maximal as well). At higher operating frequency, the ripple is at a minimum, but the output power is limited. The primary input source delivers most of the output power independently of the operating frequency: the MFC behavior is then to be incriminated. At high operating frequency, the MFC behavior perturbed though 10 Hz is still high compared to the time constant of the MFC. That phenomenon needs to be better investigated.

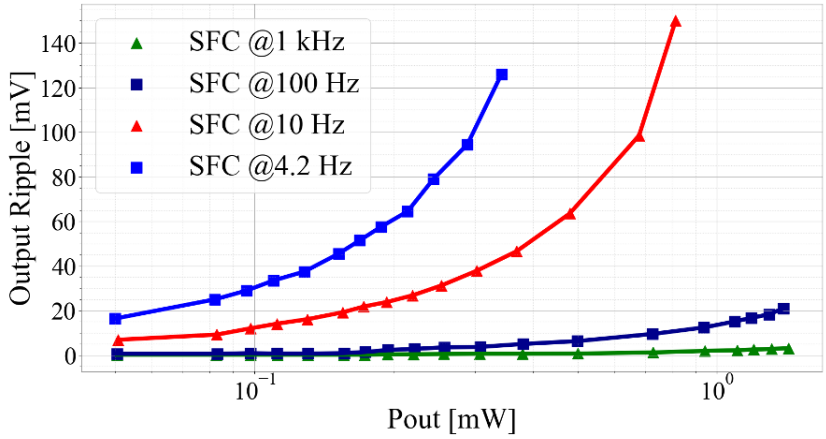

Figure 13. Impact of the operating frequency on ripple versus P_{out}.

The MFC capacitive behavior has to be investigated. A comparison is performed between an SFC and an SCC with a capacitor value of 110 µF, which is close to the MFC effective capacitance. At 10 Hz, the output voltage ripple of the SFC is lower than that of the SCC counterpart (Figure 14). The first observation is that the MFC does not behave

like a regular capacitor, even at 10 Hz, which is a frequency that is quite high compared to the MFC natural time-constant. If the output voltage ripple value is mandatory in the application, the SFC enables a higher output power that the SCC counterpart.

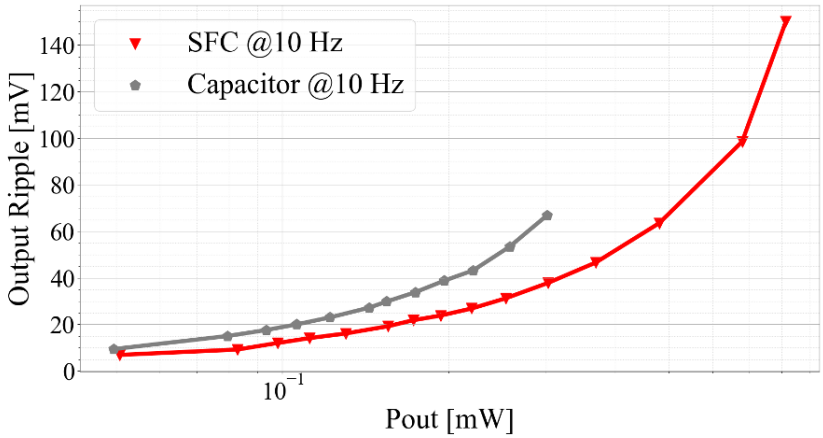

Figure 14. Output voltage ripple value versus P_{out} for equivalent SFC and SCC at 10 Hz.

5. Discussion

In [23], the authors introduced a configuration similar to the one presented here. The efficiency is 85.46% maximum, and the minimal primary voltage is 1.6 V. Figure 12 shows that a partial efficiency of more than 97% may be obtained. Moreover, the result is observed in worst-case conditions, i.e., with a low state-of-charge primary battery and an already weak MFC. The worst-case conditions may be unsuitable for the topology presented in [23].

The ratio $\eta = \frac{V_{out}}{V_{in}}$ is not sufficient to characterize an SFC. The charge exchange between the MCF and the converter should be experimentally evaluated to verify that a balance is obtained over a cycle and quantify the level of energy delivered by the MCF to the circuit for compensating losses as mentioned earlier.

The MFC presents a behavior that goes behind its capacitive aspect. It is quite fortunate that the MFC can handle operation at 10 Hz and above, although its primary time constants are not in this range of frequency. A legitimate question is whether the operating conditions are severe or not on the MCF internal phenomena. Are the operating conditions able to degrade the MFC, perturbating the bacteria film? Authors have led observations over +10 days, which may not be a sufficient time horizon to let degradation unfold. A dedicated reliability analysis is required. The MFC gives electrical energy to the system, which explains the gain in partial efficiency. The MFC alone would not be able to supply any electrical interface to produce a similar output voltage amplitude (1.6 V for an MFC of 300 mV open-circuit voltage). From that perspective, the MFC saves some energy from the primary battery. It is the essence of a range-extender function.

The cold start-up of the SFC converter has not been addressed in the paper. When using a fresh coin battery, the LM2663 starts without any issue. One area of interest is evaluating what happens if a fresh MFC is inserted in the circuit. The authors have not performed this particular test.

Three questions arise: is the benefit valid whatever the MCF topology, what primary battery lifespan is gained in the process, and how can one quantify the MFC state-of-charge prior to the end of electrical production? The worst-case condition experimented in Section 3 is sufficiently severe in terms of open-circuit voltage to authorize investigating many MFC topologies. With a gain in partial efficiency of 5% at least, it is safe to say that 5% of the primary battery lifespan is saved. Moreover, the SFC scheme enables drawing what remains of charge from the nearly exhausted primary battery. In a conventional (SCC) converter, the operation would stop for an input voltage higher than the one experimented here. There is some more energy scavenged. The state-of-charge does not apply strictly speaking to an MFC, as it is known for a battery or a hydrogen fuel cell [40,41]. On the one hand, the

level of available nutrients is not easy to evaluate. To the best of the authors' knowledge, no easy and straightforward scheme has been proposed to sense the level or density of nutrients. On the other hand, the catalytic action of microorganisms implies a varying flow of electrons, which does not simplify the measurement of the consumption of nutrients. In other words, the concept of a coulomb meter does not apply. As a consequence, there are fundamental limitations regarding a warning signal for MCF refilling with nutrients. However, it is common knowledge that a batch-mode MCF of 1 L may remain active for several months depending on the output current. Future work concerns the validation of the concept in the frame of a real, frugal, IoT system.

6. Conclusions

Quite a large number of frugal Internet-of-Thing systems are still designed using a primary energy source in the form of a non-rechargeable, tiny battery coin. Most of the systems require a DC/DC converter to adjust the battery voltage to that of the electronic part. A switched-capacitor converter is a simple, cost-effective topology. Whatever the considered topology for the capacitors in a voltage doubler, the converter features a maximum efficiency figure. The efficiency is varying quite sharply with the output power. Based on the concept of the switched-battery converter, the paper discusses the concept of a switched-fuel-cell converter where the fuel cell is a batch-mode microbial fuel cell. The SFC presents several good metrics, including the capability to operate at low frequency with a limited output voltage ripple value. As the efficiency is larger than that of an SCC counterpart, the MFC may be considered as a support to the primary battery, acting as a range extender. The gain in primary battery lifespan must be investigated within the context of a practical application.

Author Contributions: Validation, B.A.; Investigation, C.A.B. and A.P.; Writing—original draft, F.M. and B.A.; Writing—review & editing, B.A.; Visualization, F.M.; Supervision, G.P.; Project administration, G.P.; Funding acquisition, G.P. All authors have read and agreed to the published version of the manuscript.

Funding: This research received no external funding.

Data Availability Statement: No.

Conflicts of Interest: The authors declare no conflict of interest.

Abbreviations

The following abbreviations are used in this manuscript:

IoT	Internet-of-Things
IC	Integrated Circuit
MFC	Microbial Fuel Cell
MPP	Maximum Power Point
SCC	Switched-Capacitor Converter
SBC	Switched-Battery Converter
SFC	Switched-Fuel-Cell Converter

References

1. Evangelakos, E.A.; Kandris, D.; Rountos, D.; Tselikis, G.; Anastasiadis, E. Energy Sustainability in Wireless Sensor Networks: An Analytical Survey. *J. Low Power Electron. Appl.* **2022**, *12*, 65. [CrossRef]
2. Yahya, F.B.; Lukas, C.J.; Calhoun, B.H. A Top-Down Approach to Building Battery-Less Self-Powered Systems for the Internet-of-Things. *J. Low Power Electron. Appl.* **2018**, *8*, 21. [CrossRef]
3. Aiello, O. Ultra-Low-Power ICs for the Internet of Things. *J. Low Power Electron. Appl.* **2023**, *13*, 38. [CrossRef]
4. Andò, B.; Baglio, S.; Marletta, V.; Bulsara, A.R. A comparison of linear and non-linear strategies for energy harvesting from mechanical vibrations. *Front. Phys.* **2023**, *10*, 1032978. [CrossRef]
5. Torrisi, A.; Yıldırım, K.S.; Brunelli, D. Ultra-Low-Power Circuits for Intermittent Communication. *J. Low Power Electron. Appl.* **2022**, *12*, 60. [CrossRef]

6. Kozalakis, K.; Sofianidis, I.; Konstantakos, V.; Siozios, K.; Siskos, S. 73.5 µW Indoor-Outdoor Light Harvesting System with Global Maximum Power Point Tracking. *J. Low Power Electron. Appl.* **2021**, *11*, 10. [CrossRef]
7. dos Santos, P.M.; Serralheiro, A.J.; Borges, B.; Torres, J.P.N.; Charas, A. An Experimental Study on Step-Up DC/DC Converters for Organic Photovoltaic Cells. *J. Low Power Electron. Appl.* **2022**, *12*, 20. [CrossRef]
8. Caselli, M.; Ronchi, M.; Boni, A. Power Management Circuits for Low-Power RF Energy Harvesters. *J. Low Power Electron. Appl.* **2020**, *10*, 29. [CrossRef]
9. Li, S.; Zhao, Z.; Li, B.; Wei, T.; Jiang, H.; Yan, Z. Supercapacitors Accumulating Energy Harvesting from Stacked Sediment Microbial Fuel Cells and Boosting Input Power for Power Management Systems. *Int. J. Hydrogen Energy* **2022**, *47*, 10689–10700. [CrossRef]
10. Boebel, M.; Frei, F.; Blumensaat, F.; Ebi, C.; Meli, M.L.; Rüst, A. Batteryless Sensor Devices for Underground Infrastructure—A Long-Term Experiment on Urban Water Pipes. *J. Low Power Electron. Appl.* **2023**, *13*, 31. [CrossRef]
11. Evans, J.W.; Kim, B.; Ono, S.; Arias, A.C.; Wright, P.K. Multicycle Testing of Commercial Coin Cells for Buffering of Harvested Energy for the IoT. *IEEE Internet Things J.* **2021**, *8*, 10047–10051. [CrossRef]
12. Falk, M.; Shleev, S. Hybrid dual-functioning electrodes for combined ambient energy harvesting and charge storage: Towards self-powered systems. *Biosens. Bioelectron.* **2019**, *126*, 275–291. [CrossRef]
13. Naveen, K.V.; Manjunath, S.S. A reliable ultracapacitor based solar energy harvesting system for Wireless Sensor network enabled intelligent buildings. In Proceedings of the 2011 2nd International Conference on Intelligent Agent and Multi-Agent Systems, Chennai, India, 7–9 September 2011; pp. 20–25. [CrossRef]
14. Tan, Y.K. *Energy Harvesting Autonomous Sensor Systems: Design, Analysis, and Practical Implementation*; CRC Press: Boca Raton, FL, USA; Taylor & Francis Group: Abingdon, UK, 2013.
15. Tran, M.K.; Bhatti, A.; Vrolyk, R.; Wong, D.; Panchal, S.; Fowler, M.; Fraser, R. A Review of Range Extenders in Battery Electric Vehicles: Current Progress and Future Perspectives. *World Electr. Veh. J.* **2021**, *12*, 54. [CrossRef]
16. Cao, X.T.; Chung, W.Y. Range-Extended Wireless Food Spoilage Monitoring with a High Energy Efficient Battery-Free Sensor Tag. *Sens. Actuators A Phys.* **2019**, *299*, 111632. [CrossRef]
17. Mallon, K.R.; Assadian, F.; Fu, B. Analysis of On-Board Photovoltaics for a Battery Electric Bus and Their Impact on Battery Lifespan. *Energies* **2017**, *10*, 943. [CrossRef]
18. Soto, J.D.L.C.; Castillo, U.C. Fuel Cell as Range Extender in Battery Electric Vehicles for Supply Chain Fleets. In *Sustainable Supply Chain Management*; Krmac, E., Ed.; IntechOpen: Rijeka, Croatia, 2016; Chapter 4. [CrossRef]
19. Sisinni, E.; Ferrari, P.; Fernandes Carvalho, D.; Rinaldi, S.; Marco, P.; Flammini, A.; Depari, A. LoRaWAN Range Extender for Industrial IoT. *IEEE Trans. Ind. Inform.* **2020**, *16*, 5607–5616. [CrossRef]
20. Dwivedi, K.A.; Huang, S.J.; Wang, C.T.; Kumar, S. Fundamental understanding of microbial fuel cell technology: Recent development and challenges. *Chemosphere* **2022**, *288*, 132446. [CrossRef]
21. Scott, K.; Yu, E.H. *Microbial Electrochemical and Fuel Cells: Fundamentals and Applications*; Woodhead Publishing: Cambridge, UK; Elsevier: Amsterdam, The Netherlands, 2016.
22. Santoro, C.; Arbizzani, C.; Erable, B.; Ieropoulos, I. Microbial fuel cells: From fundamentals to applications. A review. *J. Power Sources* **2017**, *356*, 225–244. [CrossRef] [PubMed]
23. Prasad, J.; Tripathi, R.K. Energy Harvesting from Sediment Microbial Fuel Cell to Supply Uninterruptible Regulated Power for Small Devices. *Int. J. Energy Res.* **2019**, *43*, 2821–2831. [CrossRef]
24. Osorio de la Rosa, E.; Vázquez Castillo, J.; Carmona Campos, M.; Barbosa Pool, G.R.; Becerra Nuñez, G.; Castillo Atoche, A.; Ortegón Aguilar, J. Plant Microbial Fuel Cells–Based Energy Harvester System for Self-powered IoT Applications. *Sensors* **2019**, *19*, 1378. [CrossRef] [PubMed]
25. Koffi, N.J.; Okabe, S. High voltage generation from wastewater by microbial fuel cells equipped with a newly designed low voltage booster multiplier (LVBM). *Sci. Rep.* **2020**, *10*, 18985. [CrossRef] [PubMed]
26. Chandrarathna, S.C.; Lee, J.W. 16.8 nW Ultra-Low-Power Energy Harvester IC for Tiny Ingestible Sensors Sustained by Bio-Galvanic Energy Source. *IEEE Trans. Biomed. Circuits Syst.* **2021**, *15*, 55–67. [CrossRef]
27. Wu, W.; Zhang, D.; Fang, P. Advance in Improving the Electrical Performance of Microbial Fuel Cell. *Iop Conf. Ser. Earth Environ. Sci.* **2020**, *555*, 012004. [CrossRef]
28. Nguyen, C.L.; Tartakovsky, B.; Woodward, L. Harvesting Energy from Multiple Microbial Fuel Cells with a High-Conversion Efficiency Power Management System. *ACS Omega* **2019**, *4*, 18978–18986. [CrossRef]
29. Cheng, K.Y.; Cord-Ruwisch, R.; Ho, G. A new approach for in situ cyclic voltammetry of a microbial fuel cell biofilm without using a potentiostat. *Bioelectrochemistry* **2009**, *74*, 227–231. [CrossRef] [PubMed]
30. Lovecchio, N.; Di Meo, V.; Pietrelli, A. Customized Multichannel Measurement System for Microbial Fuel Cell Characterization. *Bioengineering* **2023**, *10*, 624. [CrossRef]
31. Wang, H.; Long, X.; Sun, Y.; Wang, D.; Wang, Z.; Meng, H.; Jiang, C.; Dong, W.; Lu, N. Electrochemical impedance spectroscopy applied to microbial fuel cells: A review. *Front. Microbiol.* **2022**, *13*, 973501. [CrossRef]
32. Zhang, H.; Martynov, K.; Li, D.; Perreault, D.J. A CMOS-Based Energy Harvesting Approach for Laterally-Arrayed Multi-Bandgap Concentrated Photovoltaic Systems. In Proceedings of the 2019 IEEE Energy Conversion Congress and Exposition (ECCE), Baltimore, MD, USA, 29 September–3 October 2019; pp. 3394–3401. [CrossRef]

33. Ferro, E.; Brea, V.M.; López, P.; Cabello, D. Micro-Energy Harvesting System Including a PMU and a Solar Cell on the Same Substrate With Cold Startup From 2.38 nW and Input Power Range up to 10 μW Using Continuous MPPT. *IEEE Trans. Power Electron.* **2019**, *34*, 5105–5116. [CrossRef]
34. Xiao, H.; Qi, N.; Yin, Y.; Yu, S.; Sun, X.; Xuan, G.; Liu, J.; Xiao, S.; Li, Y.; Li, Y. Investigation of Self-Powered IoT Sensor Nodes for Harvesting Hybrid Indoor Ambient Light and Heat Energy. *Sensors* **2023**, *23*, 3796. [CrossRef] [PubMed]
35. Recalde, C.; López, D.; Aguay, D.; García, V.J. Environmental Sensing in High-Altitude Mountain Ecosystems Powered by Sedimentary Microbial Fuel Cells. *Sensors* **2023**, *23*, 2101. [CrossRef]
36. Babauta, J.T.; Kerber, M.; Hsu, L.; Phipps, A.; Chadwick, D.B.; Arias-Thode, Y.M. Scaling up benthic microbial fuel cells using flyback converters. *J. Power Sources* **2018**, *395*, 98–105. [CrossRef]
37. Perez, E.; Berlitz, C.A.; Moursy, Y.; Allard, B.; Oukassi, S.; Pillonnet, G. Ultra-Low Frequency DC/DC Converters Using Switched Batteries. In Proceedings of the 2022 IEEE Energy Conversion Congress and Exposition (ECCE), Detroit, MI, USA, 9–13 October 2022; pp. 1–7. [CrossRef]
38. Fudim, E.V. Fundamentals of the switched-capacitor approach to circuit synthesis. *IEEE Circuits Syst. Mag.* **1984**, *6*, 12–21. [CrossRef]
39. Pereira-Rial, Ó.; Cabrini, A.; Torelli, G.; López, P.; Carrillo, J.M. Ultra-Low-Power Low-Input-Voltage Charge Pump for Micro-Energy Harvesting Applications. *IEEE Trans. Circuits Syst. I Regul. Pap.* **2022**, *70*, 154–165. [CrossRef]
40. Jin, G.; Li, L.; Xu, Y.; Hu, M.; Fu, C.; Qin, D. Comparison of SOC Estimation between the Integer-Order Model and Fractional-Order Model Under Different Operating Conditions. *Energies* **2020**, *13*, 1785. [CrossRef]
41. Duan, W.; Song, C.; Peng, S.; Xiao, F.; Shao, Y.; Song, S. An Improved Gated Recurrent Unit Network Model for State-of-Charge Estimation of Lithium-Ion Battery. *Energies* **2020**, *13*, 6366. [CrossRef]